Title

Optimal conductivity reconstruction using three-dimensional joint and model-based inversion for controlled-source and magnetotelluric data

Authors

Commer, M
Newman, GA

Publication Date

2018

Peer reviewed

Optimal conductivity reconstruction using three-dimensional joint and model-based inversion for controlled-source and magnetotelluric data

Michael Commer and Gregory A. Newman, Lawrence Berkeley National Laboratory, Berkeley, USA*

SUMMARY

The growing use of the controlled-source electromagnetic method (CSEM) for exploration applications has been driving the technical development of data acquisition, as well as three-dimensional (3D) modeling and imaging techniques. However, targeting increasingly complex geological environments also further enhances the problems inherent in large-scale inversion, such as non-uniqueness and resolution issues. In this paper, we report on two techniques to mitigate these problems. We use 3D joint CSEM and MT inversion to improve the model resolution. Further, a hybrid model parameterization approach is presented, where traditional cell-based model parameters are used simultaneously within a parametric inversion.

INTRODUCTION

Large-scale inverse problems are usually under-determined, meaning that there are more unknowns, typically in the form of digitized model meshes, than data. This adds to the problem that errors are associated with every geophysical data. The resulting issue is referred to as the problem of non-uniqueness of inverse solutions. To mitigate this problem and to improve the resolution in an inversion, it is common to take advantage of complementary natures of different geophysical datasets. In electromagnetic imaging, magnetotelluric (MT) data, providing conductivity structure information on a gross scale, can be combined with CSEM data. With the latter method responding stronger to thin resistive targets, the joint CSEM and MT inversion has the potential of limiting ambiguities in the EM data interpretation relevant to many exploration scenarios.

However, even with improved resolution capabilities, the solutions of 3D large-scale cell-based (or pixel-based) inversions with finely sampled models usually are still non-unique. Several strategies have been reported to limit the ambiguities for reconstructed targets and its conductivities. For cell-based problems, model-smoothing constraints are usually applied, limiting the solutions to a class of geologically more meaningful ones, i.e. avoiding too high conductivity contrasts. A different approach is to actually address the under-determinacy by casting the problem into a parametric problem. Usually, particular geometric shapes are assumed in parametric solutions, requiring a priori information. A model parameterization can for example be based on interfaces known from seismic reflection data. The 2D sharp-boundary inversion algorithm by Smith et al. (1999) features a parameterization with variable node-based boundaries and greatly limits the number of unknowns. Parametric inversion algorithms have also been used for the simultaneous reconstruction of both geometry and conductivity of unknown regions (Commer, 2003; Zhang et al., 2007). The obvious drawback of such methods is the necessity of sufficient background information in order to find a suitable model parameterization.

Here, we propose to use a hybrid approach, overlaying a cell-based inversion for a particular area of interest with a parametric inversion. This combines the advantages of cell-based and structure-based model parameters. We present two joint inversion examples using synthetic CSEM and MT data. The first example employs only cell-based model parameters, and simulates a survey in a marine environment. Second, we present an inversion study for a surface survey, using the hybrid parameterization approach.

METHOD

Our inversion algorithm's underlying finite-difference (FD) forward modeling algorithm for EM field simulation solves a modified form of the vector Helmholtz equation for scattered or total electric fields. The theoretical principles and numerical implementation for parallel computers are outlined in detail by Newman & Alumbaugh (1999). Details about the inversion algorithm can be found in the works of Newman & Alumbaugh (1997, 2000), and Commer & Newman (2008).

We use a non-linear conjugate gradient (NLCG) approach to minimize an objective function φ, which in principle describes how well the CSEM and MT measurements are fitted by an image produced by joint inversion. Hence, the main constituent of φ is the part describing the data misfit, φ_d. In cell-based inverse problems, in order to avoid geologically unrealistic images, φ is typically augmented by a model roughness term $\lambda\varphi_m$. This term represents an appropriate norm for measuring the model roughness. Its minimization thus enforces smooth images, acting as a stabilizer. The regularization parameter λ balances the weights of φ_d and φ_m. For a joint inverse problem, the gradient of the total objective function hence becomes

$$\nabla\varphi = \nabla\varphi_d^{CSEM} + \nabla\varphi_d^{MT} + \lambda\nabla\varphi_m , \qquad (1)$$

where the CSEM and MT data fitting errors are described by φ_d^{CSEM} and φ_d^{MT}. For the data terms, we do not employ further tradeoff parameters. One possibility of enhancing the weight of one data set is to increase the data weights, given by the reciprocals of the observation errors. In the presented synthetic studies, we use as data errors 3 %, for

CSEM, and 1 %, for MT, of the data amplitudes, both with a Gaussian distribution.

RESULTS

The first joint inversion result is summarized in Fig. 1. Here, we employ only cell-based model parameters in the traditional way. A marine CSEM-MT imaging experiment is simulated, with the true model, used for synthetic data generation, shown in Fig. 1a. The model features an air layer (z<0 m), a water layer, three seabed layers with sine-shaped boundaries, and a resistive reservoir. Synthetic measurements are calculated for 7 stations. The data consists of in-phase and quadrature components for one CSEM transmitter frequency (0.25 Hz), and the complex impedances Z_{xy} and Z_{yx} for three MT frequencies, 0.01, 0.03, and 0.07 Hz. The MT stations coincide with the CSEM source locations. Note that by using reciprocity, the simulated sail line of the CSEM transmitter represents the CSEM detector profile, here with 81 points.

Figs. 1b,c, and d show the standalone CSEM, MT, and joint CSEM-MT inversion results, respectively, after 75 NLCG iterations. While the MT method is not very sensitive to the thin resistive structure, inverting the combined data set clearly improves the standalone CSEM result by enhancing the background conductivity towards the true value within a larger model region. The reconstructed background also follows the true boundaries along a lateral extent, where the sensitivity appears to be sufficient (-2000<x<2000). The data errors, *e* in %, in Fig. 1e and f are calculated from the sum over all data points, *N*, of one given data set,

$$e = \sum_{i=1}^{N} \frac{\Delta d_i}{d_i} \cdot 100 \quad (N = N_{CSEM} \text{ or } N = N_{MT}). \quad (2)$$

The errors reflect the fact that the CSEM data set dominates the solution, which can be explained by the low sensitivity of the MT method to the resistive target. The MT data misfit of the joint inversion starts to drop below the initial value after 40 iterations, while the CSEM part is already largely reduced at this point. However, the improved reconstructed background of the image demonstrates the added value of the MT data. Usually, MT data are aquired at relatively low additional cost in real marine CSEM surveys.

The second joint inversion example simulates a surface imaging experiment, summarized in Fig. 2. The combined data set (geometry shown in Fig. 2a) consists of one CSEM profile, with one 0.25 Hz transmitter and 39 receiver points, and 15 MT stations, each with 9 impedance pairs Z_{xy} and Z_{yx}, spanning a period range of 0.1-10 s. The true model consists of 7 horizontal layers and a resistive sheet with a size of 1×1×0.2 km^3 at a depth of 1500 m below the surface. Such an imaging case might be relevant for studying the feasibility of EM monitoring in the upcoming field of geophysical monitoring of CO2 sequestration sites. Similar to 1D inversions, the regional conductivity background is described by layer-shaped model parameters, with the layer conductivities as unknowns. In this inversion, we allow 12 layer parameters, with the boundaries shown by white lines in Fig. 2b. In practice, the gradient components of all FD model cells within one given structure, here a layer, are summed up to the corresponding layer parameter's gradient component. In addition to these 12 layer parameters, the target region of interest constitutes a volume with a cell-based parameterization, adding 4500 cell parameters (Fig. 2c). Combining a parametric inversion with a cell-based inversion involves multiple choices for treating the model smoothness term in equation 1. Depending on the amount and significance of the a priori information, one might also wish to impose constraints on the structural model parameters, in order to avoid unrealistic conductivity contrasts between the layers. Here, we use smoothness constraints only within the volume of the cell-based inversion. Further, logarithmic lower (1e-3 S/m) and upper (1.5 S/m) parameter bounds (Commer & Newman, 2008) are applied to all model parameters.

The inversion results after 65 NLCG iterations for the separate and joint inversions are shown in Figs. 2d-f, using a relatively narrow color scale to focus on the target region. The combined data set clearly improves the resolution of the target zone, compared to both the separate CSEM and MT joint inversion. The misfit errors, *e* in %, calculated from equation 2 are given in the following table.

	CSEM	MT
Joint inversion	6.1	0.5
Single inversion	4.4	0.3

CONCLUSIONS

The improved resolution achieved by joint CSEM and MT inversion, owing to the complementary nature of both data types, could be demonstrated for two different synthetic data studies.

Using a parametric inversion algorithm has the advantage of greatly limiting the non-uniqueness problem. However this might come at the expense of a too strongly constrained inverse problem. Combining a parametric inversion with a cell-based approach offers to keep the structural flexibility in certain model regions of interest.

Acknowledgments

Base funding for this work was provided by the ExxonMobil Corporation and the United States Department of Energy, Office of Basic Energy Sciences, under contract DE-AC02-05CH11231.

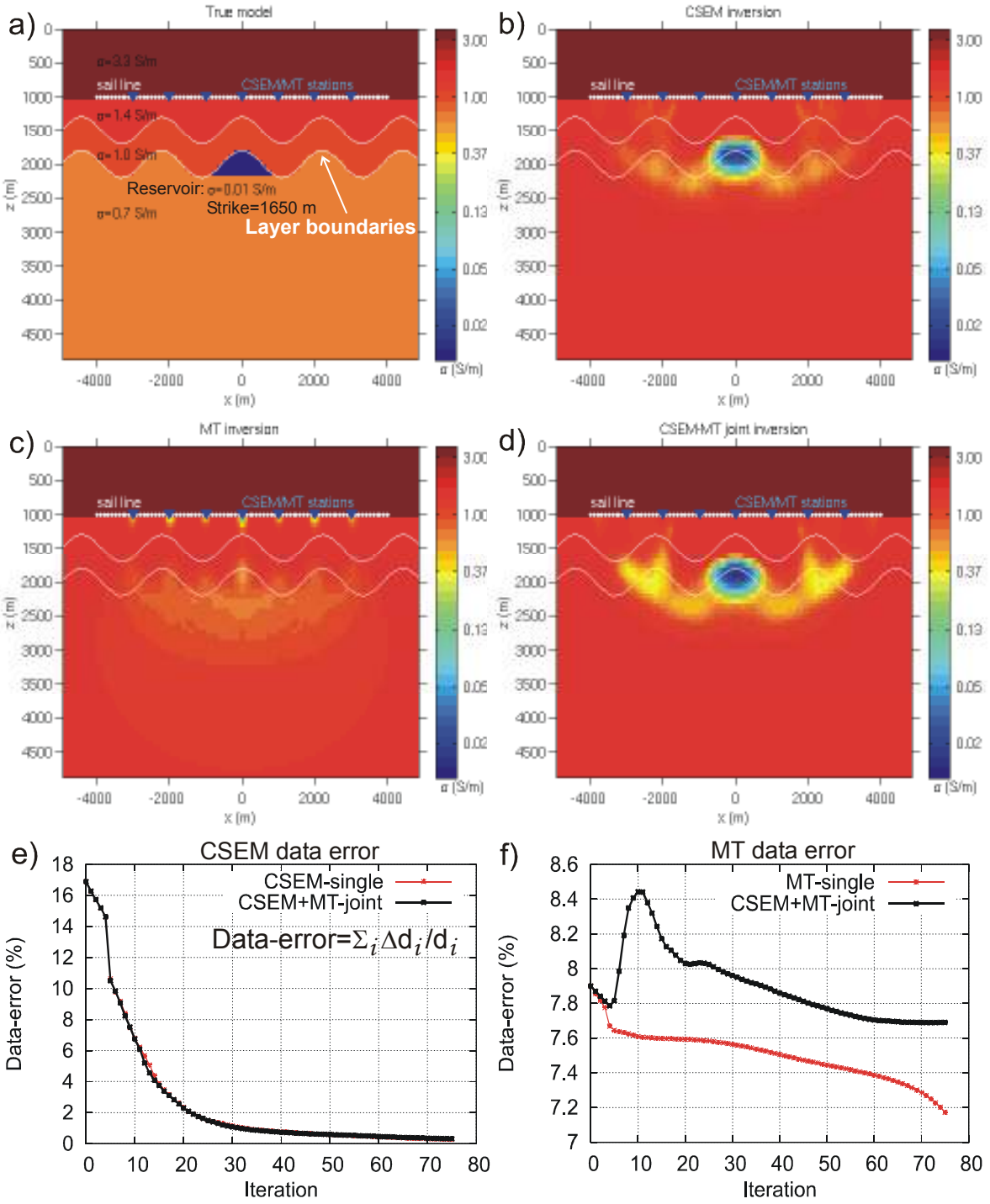

Figure 1. Marine CSEM-MT joint inversion example. a) True model used for synthetic data generation. b) CSEM inversion result. c) MT inversion result. d) CSEM-MT joint inversion result. e) and f) show the data misfit errors for the single CSEM and MT inversion (red), respectively, in comparison with the errors computed from the joint inversion result (black).

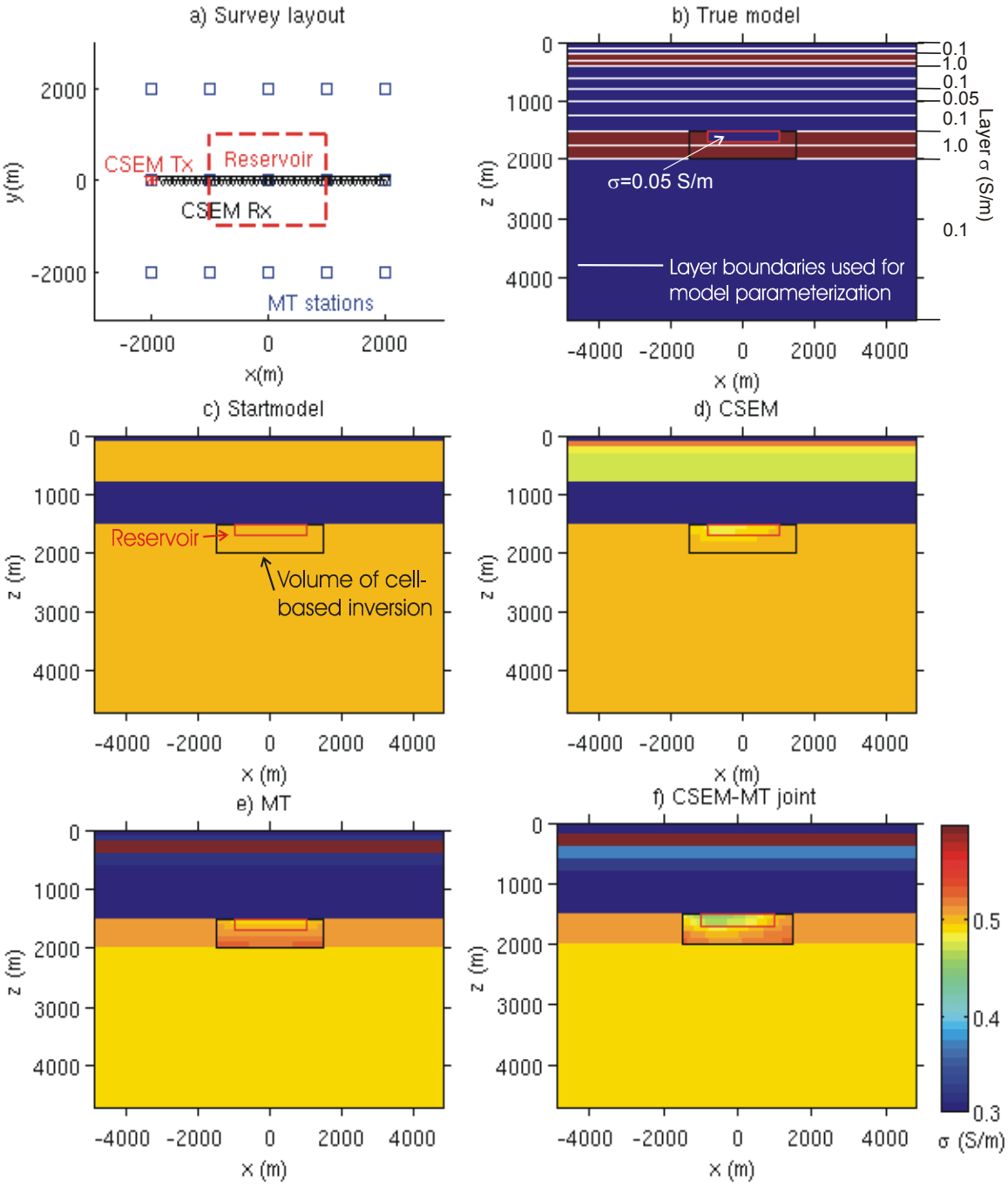

Figure 2. Surface CSEM-MT joint inversion example. a) Survey layout. b) True model with layered-model parameter boundaries (white lines). c) Start model. d) CSEM inversion result. e) MT inversion result. f) CSEM-MT joint inversion result.

EDITED REFERENCES

Note: This reference list is a copy-edited version of the reference list submitted by the author. Reference lists for the 2008 SEG Technical Program Expanded Abstracts have been copy edited so that references provided with the online metadata for each paper will achieve a high degree of linking to cited sources that appear on the Web.

REFERENCES

Commer, M., 2003, Three-dimensional inversion of transient-electromagnetic data: A comparative study: Ph.D. dissertation, University of Cologne.

Commer, M., and G. A. Newman, 2008, New advances in three-dimensional controlled-source electromagnetic inversion: Geophysical Journal International, **172**, 513–535.

Newman, G. A., and D. L. Alumbaugh, 1997, 3D massively parallel electromagnetic inversion—Part I. Theory: Geophysical Journal International, **128**, 345–354.

———1999, 3D electromagnetic modeling and inversion on massively parallel computers, *in* M. N. Oristaglio, and B. R. Spies, eds., Three-dimensional electromagnetics: SEG, 299–321.

Newman, G. A., and D. L. Alumbaugh, 2000, Three-dimensional magnetotelluric inversion using non-linear conjugate gradients: Geophysical Journal International, **140**, 410–424.

Smith, J. T., G. M. Hoversten, E. Gasperikova, and H. F. Morrioson, 1999, Sharp boundary inversion of 2D magnetotelluric data: Geophysical Prospecting, **47**, 469–486.

Zhang, Y., A. Abubakar, and T. Habashy, 2007, Model-based inversion algorithm for structural and conductivity reconstruction of marine controlled-source electromagnetic data: 23rd Annual Review of Progress Applications in Computational Electromagnetics, Expanded Abstracts, 1269–1275.